

Hourglass Dispersion and Resonance of Magnetic Excitations in the Superconducting State of the Single-Layer Cuprate $\text{HgBa}_2\text{CuO}_{4+\delta}$ Near Optimal Doping

M. K. Chan,^{1,2,*} Y. Tang,¹ C. J. Dorow,^{1,†} J. Jeong,³ L. Mangin-Thro,^{3,‡} M. J. Veit,^{1,§}

Y. Ge,^{1,||} D. L. Abernathy,⁴ Y. Sidis,³ P. Bourges,³ and M. Greven^{1,¶}

¹*School of Physics and Astronomy, University of Minnesota, Minneapolis, Minnesota 55455, USA*

²*Pulsed Field Facility, National High Magnetic Field Laboratory,*

Los Alamos National Laboratory, Los Alamos, New Mexico 87545, USA

³*Laboratoire Léon Brillouin, CEA-CNRS, CEA-Saclay, 91191 Gif sur Yvette, France*

⁴*Quantum Condensed Matter Division, Oak Ridge National Laboratory, Oak Ridge, Tennessee 37831, USA*

(Received 22 June 2016; revised manuscript received 12 September 2016; published 29 December 2016)

We use neutron scattering to study magnetic excitations near the antiferromagnetic wave vector in the underdoped single-layer cuprate $\text{HgBa}_2\text{CuO}_{4+\delta}$ (superconducting transition temperature $T_c \approx 88$ K, pseudogap temperature $T^* \approx 220$ K). The response is distinctly enhanced below T^* and exhibits a Y -shaped dispersion in the pseudogap state, whereas the superconducting state features an X -shaped (hourglass) dispersion and a further resonancelike enhancement. A large spin gap of about 40 meV is observed in both states. This phenomenology is reminiscent of that exhibited by bilayer cuprates. The resonance spectral weight, irrespective of doping and compound, scales linearly with the putative binding energy of a spin exciton described by an itinerant-spin formalism.

DOI: 10.1103/PhysRevLett.117.277002

The dynamic magnetic susceptibility of the hole-doped cuprates exhibits an hourglass-shaped (or X -shaped, upon considering an energy-momentum slice through \mathbf{q}_{AF}) spectrum centered at the two-dimensional antiferromagnetic (AF) wave vector \mathbf{q}_{AF} [1–3]. The upper dispersive branch likely results from short-range AF correlations of local moments, but the cause of the downward dispersive branch, at energies below the neck of the hourglass, has remained unclear. Results for the two cuprates most widely studied via neutron scattering, $(\text{La}, \text{Nd})_{2-x}(\text{Sr}, \text{Ba})_x\text{CuO}_4$ (La214) and $\text{YBa}_2\text{Cu}_3\text{O}_{6+\delta}$ (Y123), support contradictory scenarios. For moderately to overdoped Y123 (hole concentration $p \gtrsim 0.085$), the low-energy dispersion is accompanied by a magnetic resonance: an increase in scattering at \mathbf{q}_{AF} and energy ω_r [4,5]. Both features appear in the superconducting (SC) state and can be understood, within an *itinerant* picture, as a dispersive spin exciton bound below the particle-hole continuum and associated with the d -wave SC gap [6,7]. In contrast, La214 features an hourglass dispersion in both the SC and normal states, and no resonance in the SC state [2,8,9]. The discovery of static charge-spin “stripe” order in La214 [10] motivated an interpretation in terms of fluctuating stripes [11]. Reconciliation of these discrepancies has been further complicated by the disparate crystal structures of Y123, a double-layer cuprate (two CuO_2 layers per primitive cell), and La214, a single-layer compound.

The observation of a magnetic resonance in single-layer $\text{Ti}_2\text{Ba}_2\text{CuO}_{6+\delta}$ (Ti2201) [12] and $\text{HgBa}_2\text{CuO}_{4+\delta}$ (Hg1201) [13], which feature optimal T_c values of nearly 100 K, more than twice that of La214, raised the prospect of a

universal description of the magnetic response. However, detailed results have been difficult to obtain for these single-layer cuprates, and an hourglass dispersion has not been detected. Thus, a connection, or lack thereof, between the hourglass dispersion, the resonance, and superconductivity has not been universally established, rendering a satisfactory description of magnetic excitations of single- and double-layer cuprates elusive.

A recent study of underdoped Hg1201 (labeled HgUD71, $T_c = 71$ K) revealed a gapped Y -shaped spectrum both in the pseudogap (PG) and SC states, and no evidence for a resonance. The unusual response was attributed to strong competing PG order [14]. Since then, charge-density-wave (CDW) order in Hg1201 was found to be particularly pronounced at this doping level [15,16].

Here, we study a Hg1201 sample closer to optimal doping (HgUD88; $T_c = 88$ K), motivated by early work for optimally doped Hg1201 that yielded initial evidence for a resonance [13]. First, we confirm the observation for HgUD71 [14] that the response is enhanced below T^* and has a gapped, Y -shaped spectrum in the PG state. Whereas the large gap (about 40 meV) is unchanged in the SC state, the response of HgUD88 changes to a distinct hourglass topology and features a resonancelike enhancement at $\omega_r \approx 59$ meV. This is reminiscent of the phenomenology established for the bilayer cuprates [17,18]. The characteristic resonance energy and spectral weight scale with the particle-hole Stoner continuum threshold energy in a manner consistent with results for other cuprates, and with expectations for a spin exciton resulting from an itinerant spin formalism.

The sample, prepared following previously described procedures [14,19,20], consists of approximately 30 coaligned single crystals with a total mass of 2.8 g with full-width-at-half-maximum (FWHM) mosaic of 1.5° . Similar to Ref. [14], the value $T_c = 88$ K signifies the transition midpoint obtained by averaging uniform magnetic susceptibility data for the diamagnetic signal of the individual crystals. Measurements were performed on a time-of-flight (TOF) spectrometer [21], with the sample's crystalline c axis aligned along the incident beam, and incident neutron energies $E_i = 100$ meV (at 5 K, 100 K, and 250 K) and 130 meV (5 K). The dynamic magnetic susceptibility $\chi''(\mathbf{q}, \omega)$ was determined from the scattering intensity, calibrated to a Vanadium standard by normalizing by the anisotropic Cu^{2+} form factor [22] and the Bose population factor. The temperature dependence was measured at $(\mathbf{q}, \omega) = (\mathbf{q}_{\text{AF}}, 60$ meV) at the Laboratoire Léon Brillouin, with the 2 T triple-axes spectrometer, with fixed final energy $E_f = 35$ meV. We quote the scattering wave vector $\mathbf{Q} = H\mathbf{a}^* + K\mathbf{b}^* + L\mathbf{c}^* \equiv (H, K, L)$ in reciprocal lattice units, where $a^* = b^* = 1.62 \text{ \AA}^{-1}$ and $c^* = 0.66 \text{ \AA}^{-1}$

are the room-temperature values. Constant- ω data are fit to a Gaussian, $\chi''(\mathbf{q}, \omega) = \chi''_0 \exp\{-4 \ln 2R/(2\kappa)^2\}$, convolved with the experimental momentum resolution, where \mathbf{q} is the reduced two-dimensional wave vector, $R = |[(H - 1/2)^2 + (K - 1/2)^2]^{1/2} - \delta|^2$, 2κ the intrinsic FWHM momentum width, and δ the incommensurability away from \mathbf{q}_{AF} ; see Ref. [14] for further details.

Figures 1(a)–(j) show $\chi''(\mathbf{q})$ for select ω at $T = 5, 100,$ and 250 K. At 5 K, the gapped spectrum evolves with increasing energy from an incommensurate ring that disperses toward \mathbf{q}_{AF} and then outward again, thus exhibiting an hourglass dispersion [Fig. 1(k)]. At $T = 100$ K ($T_c + 12$ K), however, the low-energy response is commensurate with \mathbf{q}_{AF} [Figs. 1(d) and 1(i)], resulting in the Y-shaped dispersion [Fig. 1(l)] that is characteristic of the PG state [14,17,23]. Finally, at $T = 250$ K, just above $T^* \approx 220$ K [24], the response is considerably weaker than deep in the PG state.

The response at $\omega = 60$ meV [Figs. 1(c) and 1(h)], where the upward dispersion begins [Figs. 1(g), 1(k), and 1(l)], is significantly larger at 5 K than at 100 K.

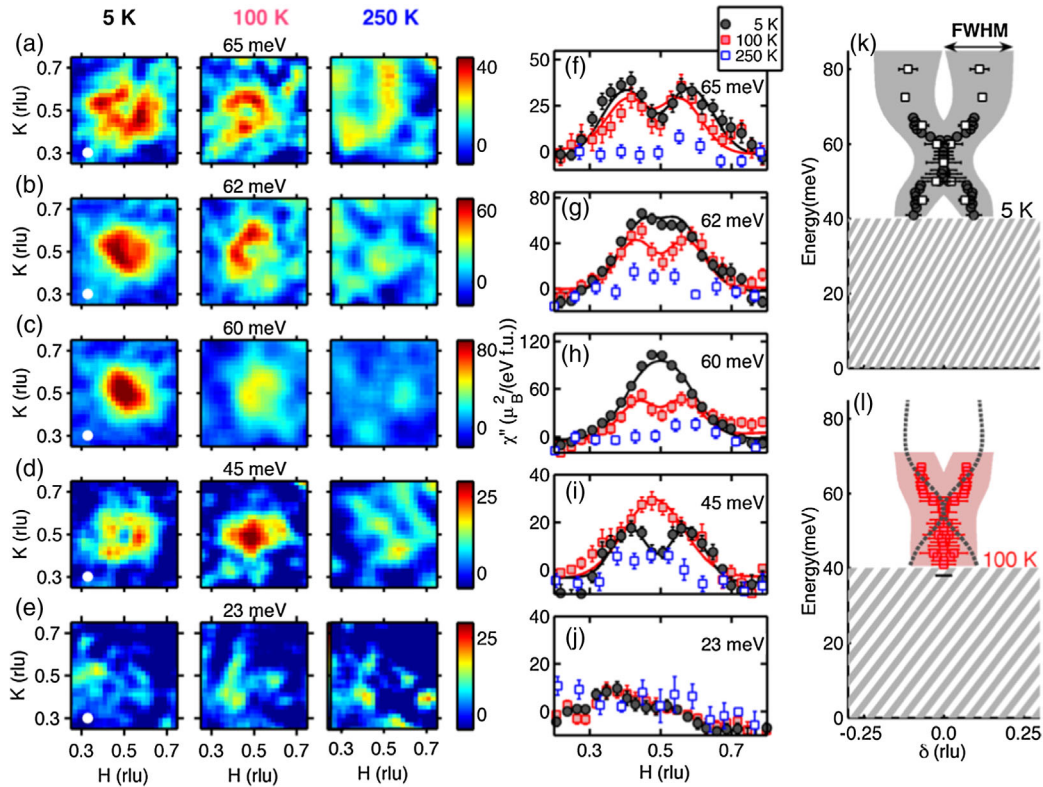


FIG. 1. (a)–(e) Constant-energy images of magnetic susceptibility at $T = 5$ K (left), 100 K (middle), and 250 K (right). Data within a 6 meV window centered at the indicated energies are averaged, except for $\omega = 23$ meV, where a 10 meV window was used. White dots (left-most panels): momentum resolution at each energy. (f)–(j) Corresponding constant-energy cuts averaged over $\{100\}$ and $\{010\}$ trajectories across \mathbf{q}_{AF} . Solid lines: Gaussian fits to data convolved with the momentum resolution. (k) Energy dependence of incommensurability δ at 5 K. Horizontal error bars: fit uncertainties for δ . Filled black circles and open squares: data taken with incident energy $E_i = 100$ meV and 130 meV, respectively. Filled gray region: FWHM of the response. Hatched area: magnetic excitation gap. (l) Energy dependence of incommensurability δ at 100 K, with dispersion at 5 K (dotted line), shown for comparison. Horizontal black bar: experimental momentum resolution at $\omega = 40$ meV.

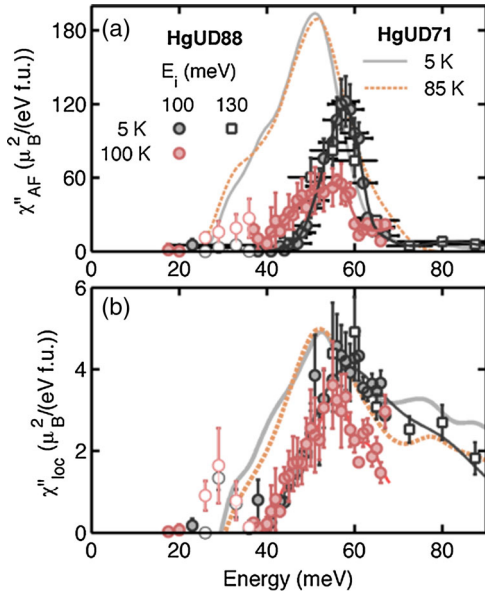


FIG. 2. (a) Energy dependence of magnetic susceptibility at \mathbf{q}_{AF} , χ''_{AF} , determined from fits to data such as those in Fig. 1 (see text). Filled circles: $E_i = 100$ meV; the data around $\omega = 30$ meV are contaminated by phonon scattering [14] and indicated by open circles. Open squares: $E_i = 130$ meV. Solid lines: guides to the eye. Horizontal bars represent the energy binning (only shown for 5 K). A large difference in χ''_{AF} is observed across T_c . In contrast, χ''_{AF} is nearly the same for HgUD71 [14] at 5 K and 85 K [gray and orange lines in (a) and (b)]. (b) Energy dependence of local susceptibility χ''_{loc} . For both HgUD88 and HgUD71 [14], the magnetic response exhibits large gaps in the PG and SC states.

This is reflected in a sharp peak at 5 K in the energy dependence of χ''_{AF} [Fig. 2(a)]. Detailed measurement of the temperature dependence of χ''_{AF} at 60 meV [Fig. 3(b)] shows a distinct increase of scattering below T^* , consistent with the result for HgUD71 [14]. However, contrary to HgUD71 [(Figs. 2(a) and 3(b))], this is followed by a further increase below T_c . We identify this feature below T_c in HgUD88 as the resonance [4,13,25].

The resonance shows a distinct enhancement in magnetic scattering below T_c in optimally and overdoped cuprates [3,13,26]. However, it is harder to discern in underdoped samples, which already exhibit significant magnetic scattering in the normal state [14,23,26], because the instrumental energy resolution is large compared to the resonance width. For HgUD88, where ω_r and hence the FWHM energy resolution of the triple-axis spectrometer are particularly large, the temperature dependence is considerably smoothed [Fig. 3(b)].

The resonance is better revealed as a peak in $\Delta\chi''_{AF} = \chi''_{AF}(5\text{ K}) - \chi''_{AF}(100\text{ K})$ [Fig. 3(a)] at $\omega_r = 59(1)$ meV, with a width that is not much larger than the resolution of the TOF spectrometer (about 5 meV FWHM). The ratio $\omega_r/(k_B T_c) = 7.9$ is the largest value reported for the cuprates [27,28]. Using $\Delta_{SC} \approx 42(2)$ meV [29,30] for the SC gap amplitude, the ratio $\omega_r/\Delta_{SC} \approx 0.70(3)$ is

consistent with the value 0.64(4), established for unconventional superconductors [28].

The present result for HgUD88 bears a striking resemblance to observations for bilayer Y123 [17,23]. The hourglass dispersion, particularly the dispersive low-energy branch, is present only below T_c , and thus, a characteristic of the SC state. Above T_c , both the resonance and its downward dispersive branch disappear, yielding a Y-shaped spectrum [31]. However, for HgUD88, the neck of the hourglass at 5 K is somewhat extended compared to other cuprates [Fig. 1(k)]. Furthermore, the upper dispersion branch extends to slightly lower energy at 100 K than at 5 K. These subtle features, established in the TOF experiment, in combination with the coarse triple-axis energy resolution used to measure the temperature dependence, might further obscure a distinct enhancement of $\chi''_{AF}(\omega_r)$ at T_c [Fig. 3(b)].

Considering the spectral weight of the resonance, $W_r = \int d\omega \Delta\chi''_{AF}$, we find $W_r = 0.54(7) \mu_B^2/\text{Cu}$ upon integrating from 51 to 64 meV. W_r can be related to ω_r . Within the itinerant picture, the interacting spin susceptibility is computed using the random phase approximation. In the SC state, the resonance at \mathbf{q}_{AF} is part of a spin exciton, i.e., a spin-triplet collective mode bound below the threshold of the Stoner continuum ω_c [7,32]. The resonance weight is linearly related to the reduced binding energy, $(\omega_c - \omega_r)/\omega_c$, by $W_r \approx (g\mu_B)^2 2\pi(V^2\beta)^{-1}(\omega_c - \omega_r)/\omega_c$, where V is the planar interaction that enhances the bare susceptibility, and $g = 2$ is the Landé factor. The quantities ω_c and β are related to the hot spots (hs), defined as Fermi-surface points connected by \mathbf{q}_{AF} : $\beta = 4/(\pi\nu_{hs}\nu_{hs+Q_{AF}} \sin(\Theta_{hs}))$, where ν_{hs} and $\nu_{hs+Q_{AF}}$ are the Fermi velocities at the hot spots and Θ_{hs} is the angle between their directions; ω_c at the hot spots is estimated as $1.8\Delta_{SC}$ [33], where $\Delta_{SC} \approx 42(2)$ meV [29,30]. As shown in Fig. 3(c), upon combining our result for HgUD88 with those for Y123 [33], $\text{Bi}_2\text{Sr}_2\text{CaCu}_2\text{O}_{8+\delta}$ (Bi2212) [25] and Tl2201 [12], we find remarkably good linear scaling with zero intercept between W_r and the reduced binding energy. The common scaling factor implies universal band structure and interaction parameters, within the experimental error, for different cuprate families and hole concentrations.

Alternatively, the resonance has been attributed to a redistribution of spectral weight of local spin fluctuations from energies below to energies above a spin gap that appears in the SC state [11,35]. The gap in HgUD88 is apparent from the lack of low-energy magnetic scattering [Figs. 1(e) and 1(j)]. To better determine the gap size, we examine the local susceptibility, $\chi''_{loc}(\omega) = \int \chi''(\mathbf{Q}, \omega) d^2\mathbf{q} / \int d^2\mathbf{q}$ (integration over the AF Brillouin zone). As seen from Fig. 2(b), HgUD88 features a particularly large gap of about 40 meV in both the PG and SC states. With increasing temperature, the strength of magnetic excitations decreases, yet the gap does not close. Consistent with the result for HgUD71 [14], the gap is a property of the PG and not the SC

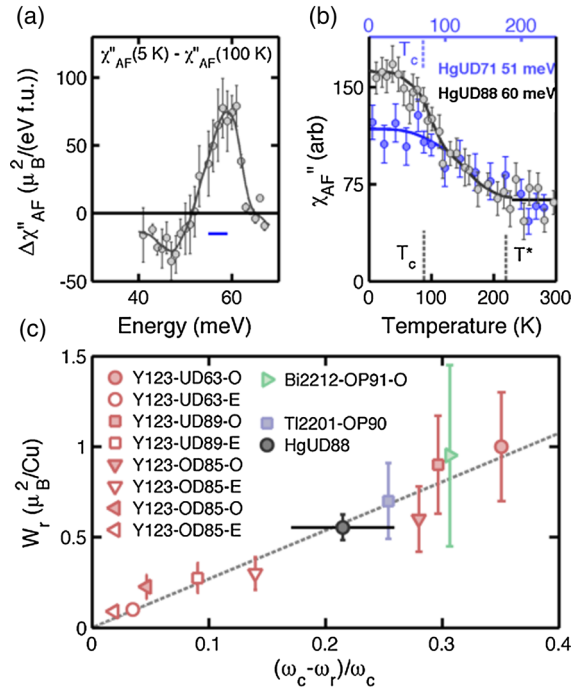


FIG. 3. (a) Change of χ''_{AF} across T_c . Horizontal blue bar: FWHM energy resolution. The large peak at $\omega_r = 59 \pm 1$ meV is the magnetic resonance. (b) Temperature dependence of χ''_{AF} at $\omega \approx \omega_r$ (black) measured with a triple-axis spectrometer, with FWHM energy resolution ≈ 10 meV. T_c and T^* (interpolated from planar transport measurements [24]) are indicated by the black dashed vertical lines. In contrast to HgUD88, the magnetic response of HgUD71 (blue) saturates in the SC state (from Ref. [14]); the temperature axis (top) is scaled to match T_c for HgUD71 with T_c for HgUD88. (c) W_r as a function of $(\omega_c - \omega_r)/\omega_c$ for numerous cuprates. The linear scaling and zero intercept (dashed line) are consistent with a spin-exciton description of the resonance [33]. Y123 [33,34] and Bi2212 [25] are bilayer cuprates and thus exhibit odd- and even-parity resonances, whereas single-layer TI2201 [12] and Hg1201 (HgUD88, present work) feature only one resonance mode. Labels indicate the hole concentrations corresponding to underdoped (UD), optimally doped (OP), and overdoped (OD) regimes, followed by numbers designating T_c and, if relevant, even (E) and odd (O) resonance modes.

state [26,35]. We thus cannot attribute the resonance to a spectral weight redistribution due to the opening of a gap. Although prior neutron scattering work yielded evidence for a “spin pseudogap” [4,14,27,36], the present result constitutes the clearest and largest manifestation of such a gap.

The spin-exciton scenario can semiquantitatively account for (i) the magnitude of the resonance and (ii) its connection to a downward dispersing mode in the SC state of HgUD88. However, it fails to explain the absence of both features in HgUD71 [14]. It is interesting to compare the two-particle spectra in the charge and spin sectors, probed by electronic Raman scattering (ERS) and neutron scattering, respectively. In ERS, the hallmark of the SC state is the pair-breaking peak in the B_{1g} channel, which probes

the antinodal regions of the Fermi surface that are approximately spanned by \mathbf{q}_{AF} . The magnitude of this peak decreases with decreasing doping. Thus, while the pair-breaking peak is sizable in HgUD88, it is much weaker in HgUD71, and disappears at lower doping [30,37,38]. This phenomenon could be ascribed to the vanishing of coherent Bogoliubov quasiparticles because at lower doping, an increasing portion of the Fermi surface is dominated by the PG. Furthermore, CDW order is particularly prominent in underdoped Hg1201, with $T_c \approx 70$ K [15,16], which contributes to the destruction of quasiparticle coherence on portions of the Fermi surface connected by the CDW wavevector.

Our results establish that excitations across the Fermi surface in the presence of either SC and/or PG order should be considered in accounting for the magnetic spectrum in both double- and single-layer cuprates. Recent transport measurements indicate Fermi-liquid behavior in the PG state [24,39,40], which adds further support for the need to pursue such formulations. However, the spin-exciton scenario can, in principle, only generate a single pole (below the Stoner continuum) at each \mathbf{Q} , and thus this scenario cannot account for both the downward and upward dispersive branches. In addition to the pair-breaking peak in the ERS B_{1g} channel, a two-magnon peak is observed [30], which indicates the persistence of short-range local-moment AF correlations, likely associated with the upward dispersive part of the spectrum. A theoretical approach that incorporates both itinerant and local spins, such as in Ref. [41], might thus be necessary. Understanding the Y-shaped spectrum and the large spin gap will likely require the consideration of the relationship between the magnetic degrees of freedom and the experimentally detected broken symmetry states [16,42–46] in the PG state.

It has been proposed that spin-fluctuation mediated pairing is the common thread linking a broad class of unconventional superconductors [47]. In the case of the cuprates, AF correlations have been argued to be the cause not only of the d -wave superconductivity, but also of the PG phenomena [48–50]. We have established a phenomenology of the magnetic response in the PG and SC states that is common to single- and double-layer compounds, namely a Y-shaped PG spectrum that evolves into an X-shaped (hourglass) response, accompanied by a resonance in the SC state. Based on general considerations, the magnetic resonance is associated with a SC gap function that undergoes a sign change, which is naturally the case in a Fermi-liquid picture for the d -wave cuprates [28]. In the La-based cuprates, the magnetic response does not undergo a change from X- to Y-shaped at T_c . However, the low-energy incommensurability was found to decrease slowly with increasing temperature, e.g., from $\delta \approx 0.12$ at 8 K to 0.08 at 200 K in $\text{La}_{1.875}\text{Ba}_{0.125}\text{CuO}_4$ [51]. It is tempting to attribute this to preformed SC pairs, which have been

argued to appear at high temperatures in the La-based cuprates [52]. However, the lack of a \mathbf{q}_{AF} resonance, the prominence of stripe correlations [11], and recent experiments indicating a narrow SC fluctuation range above T_c [53–55] indicate the proximity of a stripe instability in this particular cuprate family as the dominating factor that determines their low-energy magnetic spectrum.

We thank Andrey Chubukov, Yuan Li and Guichuan Yu for comments on the manuscript. This work was funded by the Department of Energy through the University of Minnesota Center for Quantum Materials, under DE-FG02-06ER46275 and DE-SC-0006858, and through Award No. LANLF100. LLB is supported by UNESCOS (Contract No. ANR-14-CE05-0007) and NirvAna (Contract No. ANR-14-OHRI-0010) of the ANR. ORNL's SNS is sponsored by the Scientific User Facilities Division, Office of Basic Energy Sciences, US Department of Energy.

*mkchan@lanl.gov

[†]Present address: Department of Physics, University of California, San Diego, 9500 Gilman Drive La Jolla, CA 92093, USA.

[‡]Present address: Institute Laue Langevin, Grenoble 38042 CEDEX 9, France.

[§]Present address: Department of Applied Physics, Stanford University, Stanford, CA 94305, USA.

^{||}Present address: Department of Physics, Penn State University, University Park, PA 16802, USA.

[¶]greven@umn.edu

- [1] D. Reznik, P. Bourges, L. Pintschovius, Y. Endoh, Y. Sidis, T. Masui, and S. Tajima, *Phys. Rev. Lett.* **93**, 207003 (2004).
- [2] J. M. Tranquada, H. Woo, T. G. Perring, H. Goka, G. D. Gu, and G. Xu, *Nature (London)* **429**, 534 (2004).
- [3] S. Pailhès, Y. Sidis, P. Bourges, V. Hinkov, A. Ivanov, C. Ulrich, L. P. Regnault, and B. Keimer, *Phys. Rev. Lett.* **93**, 167001 (2004).
- [4] J. Rossat-Mignod, L. Regnault, C. Vettier, P. Bourges, P. Burlat, and J. Bossy, *Physica (Amsterdam)* **185C**, 86 (1991).
- [5] H. A. Mook, M. Yethiraj, G. Aeppli, T. E. Mason, and T. Armstrong, *Phys. Rev. Lett.* **70**, 3490 (1993).
- [6] F. Onufrieva and P. Pfeuty, *Phys. Rev. B* **65**, 054515 (2002).
- [7] M. Eschrig, *Adv. Phys.* **55**, 47 (2006).
- [8] O. J. Lipscombe, B. Vignolle, T. G. Perring, C. D. Frost, and S. M. Hayden, *Phys. Rev. Lett.* **102**, 167002 (2009).
- [9] M. Fujita, H. Hiraka, M. Matsuda, M. Matsuura, J. M. Tranquada, S. Wakimoto, G. Xu, and K. Yamada, *J. Phys. Soc. Jpn.* **81**, 011007 (2012).
- [10] J. M. Tranquada, B. J. Sternlieb, J. D. Axe, Y. Nakamura, and S. Uchida, *Nature (London)* **375**, 561 (1995).
- [11] S. A. Kivelson, I. P. Bindloss, E. Fradkin, V. Oganesyan, J. M. Tranquada, A. Kapitulnik, and C. Howald, *Rev. Mod. Phys.* **75**, 1201 (2003).
- [12] H. He, P. Bourges, Y. Sidis, C. Ulrich, L. P. Regnault, S. Pailhès, N. S. Berzigiarova, N. N. Kolesnikov, and B. Keimer, *Science* **295**, 1045 (2002).
- [13] G. Yu, Y. Li, E. M. Motoyama, X. Zhao, N. Barišić, Y. Cho, P. Bourges, K. Hradil, R. A. Mole, and M. Greven, *Phys. Rev. B* **81**, 064518 (2010).
- [14] M. K. Chan, C. J. Dorow, L. Mangin-Thro, Y. Tang, Y. Ge, M. J. Veit, G. Yu, X. Zhao, A. D. Christianson, J. T. Park, Y. Sidis, P. Steffens, D. L. Abernathy, P. Bourges, and M. Greven, *Nat. Commun.* **7**, 10819 (2016).
- [15] J. P. Hinton *et al.*, *Sci. Rep.* **6**, 23610 (2016).
- [16] W. Tabis *et al.*, *Nat. Commun.* **5**, 5875 (2014).
- [17] P. Bourges, Y. Sidis, H. F. Fong, L. P. Regnault, J. Bossy, A. Ivanov, and B. Keimer, *Science* **288**, 1234 (2000).
- [18] B. Fauqué, Y. Sidis, L. Capogna, A. Ivanov, K. Hradil, C. Ulrich, A. I. Rykov, B. Keimer, and P. Bourges, *Phys. Rev. B* **76**, 214512 (2007).
- [19] X. Zhao, G. Yu, Y.-C. Cho, G. Chabot-Couture, N. Barišić, P. Bourges, N. Kaneko, Y. Li, L. Lu, E. M. Motoyama, O. P. Vajk, and M. Greven, *Adv. Mater.* **18**, 3243 (2006).
- [20] N. Barišić, Y. Li, X. Zhao, Y.-C. Cho, G. Chabot-Couture, G. Yu, and M. Greven, *Phys. Rev. B* **78**, 054518 (2008).
- [21] D. L. Abernathy, M. B. Stone, M. J. Logiullo, M. S. Lucas, O. Delaire, X. Tang, J. Y. Y. Lin, and B. Fultz, *Rev. Sci. Instrum.* **83**, 015114 (2012).
- [22] S. Shimoto, M. Sato, J. M. Tranquada, B. J. Sternlieb, and G. Shirane, *Phys. Rev. B* **48**, 13817 (1993).
- [23] V. Hinkov, P. Bourges, S. Pailhès, Y. Sidis, A. Ivanov, C. D. Frost, T. G. Perring, C. T. Lin, D. P. Chen, and B. Keimer, *Nat. Phys.* **3**, 780 (2007).
- [24] N. Barišić, M. K. Chan, Y. Li, G. Yu, X. Zhao, M. Dressel, A. Smontara, and M. Greven, *Proc. Natl. Acad. Sci. U.S.A.* **110**, 12235 (2013).
- [25] H. F. Fong, P. Bourges, Y. Sidis, L. P. Regnault, A. Ivanov, G. D. Gu, N. Koshizuka, and B. Keimer, *Nature (London)* **398**, 588 (1999).
- [26] P. Dai, H. A. Mook, R. D. Hunt, and F. Doğan, *Phys. Rev. B* **63**, 054525 (2001).
- [27] P. Bourges, B. Keimer, S. Pailhès, L. P. Regnault, Y. Sidis, and C. Ulrich, *Physica (Amsterdam)* **424C**, 45 (2005).
- [28] G. Yu, Y. Li, E. M. Motoyama, and M. Greven, *Nat. Phys.* **5**, 873 (2009).
- [29] I. M. Vishik, N. Barišić, M. K. Chan, Y. Li, D. D. Xia, G. Yu, X. Zhao, W. S. Lee, W. Meevasana, T. P. Devereaux, M. Greven, and Z. X. Shen, *Phys. Rev. B* **89**, 195141 (2014).
- [30] Y. Li, M. LeTacon, Y. Matiks, A. V. Boris, T. Loew, C. T. Lin, L. Chen, M. K. Chan, C. Dorow, L. Ji, N. Barišić, X. Zhao, M. Greven, and B. Keimer, *Phys. Rev. Lett.* **111**, 187001 (2013).
- [31] In the normal state of Y123, the low-energy response is only commensurate along \mathbf{b}^* . The response along \mathbf{a}^* is still incommensurate, albeit with an incommensurability that is smaller than in the SC state [23]. This is in contrast to the low-energy response in HgUD71 [14] and HgUD88, which is commensurate and isotropic.
- [32] A. J. Millis and H. Monien, *Phys. Rev. B* **54**, 16172 (1996).
- [33] S. Pailhès, C. Ulrich, B. Fauqué, V. Hinkov, Y. Sidis, A. Ivanov, C. T. Lin, B. Keimer, and P. Bourges, *Phys. Rev. Lett.* **96**, 257001 (2006).
- [34] H. F. Fong, P. Bourges, Y. Sidis, L. P. Regnault, J. Bossy, A. Ivanov, D. L. Milius, I. A. Aksay, and B. Keimer, *Phys. Rev. B* **61**, 14773 (2000).

- [35] C. Stock, W. J. L. Buyers, R. Liang, D. Peets, Z. Tun, D. Bonn, W. N. Hardy, and R. J. Birgeneau, *Phys. Rev. B* **69**, 014502 (2004).
- [36] C. H. Lee, K. Yamada, H. Hiraka, C. R. Venkateswara Rao, and Y. Endoh, *Phys. Rev. B* **67**, 134521 (2003).
- [37] M. LeTacon, A. Sacuto, A. Georges, G. Kotliar, Y. Gallais, D. Colson, and A. Forget, *Nat. Phys.* **2**, 537 (2006).
- [38] Y. Li, M. LeTacon, M. Bakr, D. Terrade, D. Manske, R. Hackl, L. Ji, M. K. Chan, N. Barišić, X. Zhao, M. Greven, and B. Keimer, *Phys. Rev. Lett.* **108**, 227003 (2012).
- [39] M. K. Chan, M. J. Veit, C. J. Dorow, Y. Ge, Y. Li, W. Tabis, Y. Tang, X. Zhao, N. Barić, and M. Greven, *Phys. Rev. Lett.* **113**, 177005 (2014).
- [40] S. Mirzaei, D. Stricker, J. Hancock, C. Berthod, A. Georges, E. van Heumen, M. K. Chan, X. Zhao, Y. Li, M. Greven, N. Barišić, and D. van der Marel, *Proc. Natl. Acad. Sci. U.S.A.* **110**, 5774 (2013).
- [41] M. V. Eremin, I. M. Shigapov, and I. M. Eremin, *Eur. Phys. J. B* **85**, 131 (2012).
- [42] A. Kaminski *et al.*, *Nature (London)* **416**, 610 (2002).
- [43] B. Fauqué, Y. Sidis, V. Hinkov, S. Pailhès, C. T. Lin, X. Chaud, and P. Bourges, *Phys. Rev. Lett.* **96**, 197001 (2006).
- [44] Y. Li, V. Balédent, N. Barišić, Y. Cho, B. Fauqué, Y. Sidis, G. Yu, X. Zhao, P. Bourges, and M. Greven, *Nature (London)* **455**, 372 (2008).
- [45] J. Xia, E. Schemm, G. Deutscher, S. A. Kivelson, D. A. Bonn, W. N. Hardy, R. Liang, W. Siemons, G. Koster, M. M. Fejer, and A. Kapitulnik, *Phys. Rev. Lett.* **100**, 127002 (2008).
- [46] G. Ghiringhelli, M. LeTacon, M. Minola, S. Blanco-Canosa, C. Mazzoli, N. B. Brookes, G. M. D. Luca, A. Frano, D. G. Hawthorn, F. He, T. Loew, M. M. Sala, D. C. Peets, M. Salluzzo, E. Schierle, R. Sutarto, G. A. Sawatzky, E. Weschke, B. Keimer, and L. Braicovich, *Science* **337**, 821 (2012).
- [47] D. J. Scalapino, *Rev. Mod. Phys.* **84**, 1383 (2012).
- [48] K. B. Efetov, H. Meier, and C. Pépin, *Nat. Phys.* **9**, 442 (2013).
- [49] Y. Wang and A. V. Chubukov, *Phys. Rev. B* **90**, 035149 (2014).
- [50] A. Allais, J. Bauer, and S. Sachdev, *Phys. Rev. B* **90**, 155114 (2014).
- [51] M. Fujita, H. Goka, K. Yamada, J. M. Tranquada, and L. P. Regnault, *Phys. Rev. B* **70**, 104517 (2004).
- [52] Z. A. Xu, N. P. Ong, Y. Wang, T. Kakeshita, and S. Uchida, *Nature (London)* **406**, 486 (2000).
- [53] O. Cyr-Choinière, R. Daou, F. Laliberte, D. LeBoeuf, N. Doiron-Leyraud, J. Chang, J.-Q. Yan, J.-G. Cheng, J.-S. Zhou, J. B. Goodenough, S. Pyon, T. Takayama, H. Takagi, Y. Tanaka, and L. Taillefer, *Nature (London)* **458**, 743 (2009).
- [54] M. S. Grbić, N. Barišić, A. Dulčić, I. Kupčić, Y. Li, X. Zhao, G. Yu, M. Dressel, M. Greven, and M. Požek, *Phys. Rev. B* **80**, 094511 (2009).
- [55] L. S. Bilbro, R. V. Aguilar, G. Logvenov, O. Pelleg, I. Božović, and N. P. Armitage, *Nat. Phys.* **7**, 298 (2011).